Synthesis, Structure and Magnetic Properties of a Series of Novel Isophthalate-Bridged Manganese(II) Polymers with Double-Layer or Double-Chain Structures

Chengbing Ma,[a,d] Changneng Chen,[a] Qiutian Liu,*[a] Feng Chen,[a] Daizheng Liao,[b] Licun Li,[b] and Licheng Sun[c]

Keywords: Manganese / Crystal structure / Isophthalic acid / Magnetic properties / Structural topology

Four isophthalate-bridged manganese(II) coordination polymers, $[Mn_4(ip)_4(H_2O)_2(Him)_4]_n$ (**1**), $[Mn(ip)(Him)_2]_n$ (**2**), $[Mn(ip)(dpe)]_n{\cdot}0.5ndpe\cdot n H_2O$ (**3**) and $[Mn_2(ip)_2(bpy)_2]_n$ (**4**) [ip = isophthalate, Him = imidazole, bpy = 2,2′-bipyridine and dpe = (*E*)-1,2-bis(4-pyridyl)ethene], have been rationally synthesized and characterized by single-crystal X-ray structure determinations and magnetic studies. Both **1** and **3** are two-dimensional (2D) double-layer polymers. In **1**, novel Mn_4 entities are linked by ip ligands, while **3** is made of $[Mn(ip)]_n$ parallel double chains cross-linked by the μ-dpe ligands. Both **2** and **4** are one-dimensional (1D) double-chain polymers, where **2** is composed of $[Mn(ip)]_n$ parallel double chains capped by the Him ligands, while **4** is made of $[Mn_2(ip)_2]_n$ helical double chains capped by the chelating bpy ligands. Variable-temperature magnetic susceptibility measurements revealed weak antiferromagnetic exchange interactions between the adjacent Mn^{II} ions of the four coordination polymers. The data of **2**–**4** were fitted to the homonuclear alternating chain model to give magnetic coupling parameters of $J_1 = -0.71(4)$ to $-1.01(3)$ cm^{-1} and $J_2 = -0.02(2)$ to $-0.46(2)$ cm^{-1}. In the case of **1**, the fitting of magnetic data considering only the interactions within the Mn_4 moiety led to $J = -2.17(1)$ cm^{-1} and $zJ' = -0.01(5)$ cm^{-1}, using a combination of a dimeric model and a mean molecular field approximation model.

Introduction

Currently, there is great interest in metal-organic hybrid materials containing paramagnetic metal ions within extended structures. This is driven to a large extent by their fascinating network topologies and potential application in the field of molecular magnetism.[1,2] The low-dimensional (1D chain-like or 2D layer-like) extended structures have attracted special interest on account of their specific structural features and unusual nonlinear optical and magnetic properties.[3] Therefore, rational design and construction of new materials with specific network structures and investigation of their properties have become a particularly important and topical subject. One commonly used strategy to construct such extended networks is to select appropriate bridging ligands which can transmit magnetic interactions in addition to binding several metal ions in a specific coordination geometry. Accordingly, polycarboxylic acid ligands are good candidates for this purpose. The three isomeric benzenedicarboxylic acids, i.e. phthalic acid, isopthalic acid and terephthalic acid, are especially suitable since they can bind metal ions in a variety of modes and can provide various superexchange pathways, which transmit magnetic interactions between metal ions through either the carboxylate group or the benzene ring of the ligand. Among these three isomeric dicarboxylates, major studies performed using terephthalate resulted in a rich variety of complexes with interesting structures and various magnetic properties.[4] The other two isomers have not been studied extensively for this purpose.[5,6]

On the other hand, the manganese(II) carboxylate complexes have long been of special interest since they are known to exist at the active sites of some metalloenzymes.[7] As part of our ongoing work on manganese complexation by dicarboxylic acids,[8] we have explored the reaction systems containing the Mn^{2+} ion and the isomeric benzenedicarboxylic acids as primary bridging ligand, paying par-

[a] State Key Laboratory of Structural Chemistry, Fujian Institute of Research on the Structure of Matter, Chinese Academy of Sciences,
Fuzhou 350002, China
Fax: (internat.) + 86-591-3714946
E-mail: lqt@ms.fjirsm.ac.cn
[b] Department of Chemistry, Nankai University,
Tianjin, China
[c] State Key Laboratory of Fine Chemicals, Dalian University of Technology,
Dalian, China
[d] Graduate School of the Chinese Academy of Sciences,
Beijing, China

  DOI: 10.1002/ejic.200400095

ticular attention to rational design of the magnetically coupled complexes with specific polymeric frameworks. Concurrently, introduction into the reaction systems of diimine chelating ligands, such as 2,2′-bipyridine and 1,10-phenanthroline, imidazole or linear ditopic ligands, such as 4,4′-bipyridine and (*E*)-1,2-bis(4-pyridyl)ethene, as ancillary ligands, was expected to inhibit the expansion of polymeric frameworks in order to obtain the desired low-dimensional polymers, or to induce the evolution of novel structures.

In this work, we report a novel family of Mn^{2+} coordination polymers **1**−**4**. They were isolated by treatment of an Mn^{2+} salt with isophthalic acid in the presence of selected ancillary ligands − imidazole, (*E*)-1,2-bis(4-pyridyl)ethene and 2,2′-bipyridine, under different crystallization conditions (Scheme 1). Single-crystal X-ray diffraction analyses revealed either double-chain structures or double-layer structures, which differ substantially from those of several metal isophthalate polymeric compounds reported previously.[5,9] The isophthalate ligands display various coordination modes (Scheme 2) and mediate overall antiferromagnetic exchange interactions between Mn^{2+} ions in these coordination polymers.

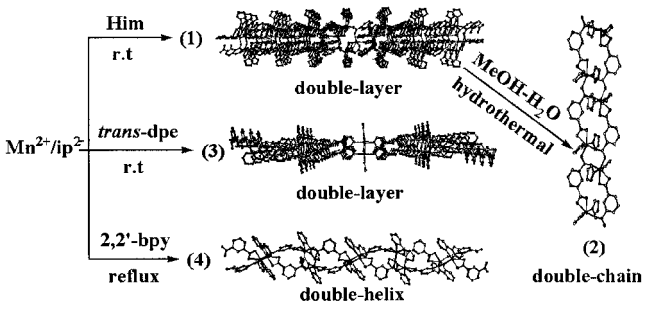

Scheme 1

Results and Discussion

Preparation of the Complexes and IR Spectroscopy

When compared with the manganese complexes containing monocarboxylate ligands such as acetate, benzoate and their derivatives, the structural information for manganese dicarboxylate complexes is relatively scarce. This is mainly because of the insolubility of the polymeric materials resulted from the reaction of a dicarboxylate with an Mn^{2+} salt under ambient conditions. The reaction of isophthalate with Mn^{2+} salts in the presence of imidazole is an exception, resulting in a clear solution. Cosolvent methanol was added in order to promote crystallization of **1**. As indicated in the structural description of **1** given below, only three of the four carboxyl O atoms in the isophthalate ligand (see b in Scheme 2) are coordinated and there is a relatively rare aqua coordination to the metal ion. The unexpected ancillary ligation by water often results in poor control over the framework of the final product. The fact that hydrothermal reaction can enhance metal−ligand interactions rather than metal−water coordination has been clearly demonstrated in several cases.[10] Further study of the reaction of **1** in an H_2O/CH_3OH solvent mixture under hydrothermal conditions led to deposition of **2**, in which metal−water coordination was blocked and all of the carboxyl O atoms take part in coordination (see c in Scheme 2). Taking into account that formation of higher dimensionality systems is prevented by the axially capping imidazole ligands in the 1D chain structure of **2**, the coordination polymer **3**, possessing a 2D layer structure, was expected with confidence when the linear *exo*-bidentate (*E*)-1,2-bis(4-pyridyl)ethene ligand was used in place of the axial imidazole ligands. The near parallel double-chain of $[Mn(ip)]_n$ in **2** was modified to a distorted double-helical chain of $[Mn_2(ip)_2]_n$ in **4** by means of *cis* chelation of the rigid 2,2′-bipyridine ligand used in place of the imidazole ligand.

IR spectra of the coordination polymers offer some valuable information about both the presence of isophthalate and the coordination modes of the carboxylates. The absence of any strong absorptions around 1700 cm^{-1} indicates that all carboxyl groups in **1**−**4** are deprotonated. Of three strong characteristic peaks at 1566, 1448 and 1394 cm^{-1} for **1**, the one at 1566 cm^{-1} is attributed to $\nu_{as}(COO)$ of all the carboxylate groups, while the peaks at 1448 cm^{-1} and 1394 cm^{-1} may be assigned to $\nu_s(COO)$ of the bidentate carboxylate group and the monodentate carboxylate group, respectively, since it is known that the difference $\Delta = \nu_{as} - \nu_s$ is smaller in the former (118 cm^{-1}) than in the latter (172

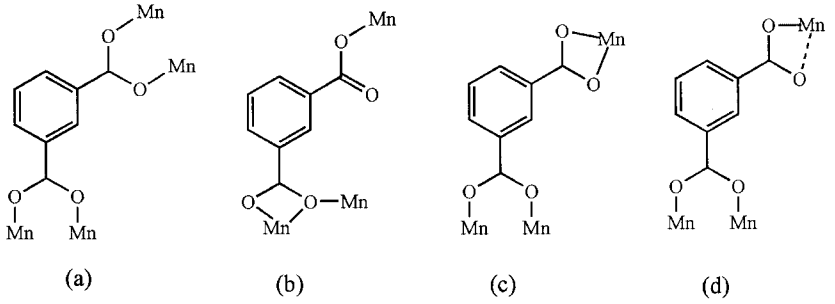

Scheme 2. Coordination modes of isophthalate found in this work: (a) bridging bis(bidentate) μ_4-mode, (b) bridging/chelating bidentate and monodentate μ_3-mode, (c) bridging and chelating bis(bidentate) μ_3-mode, and (d) bridging bidentate and monodentate μ_3-mode

cm^{-1}).[11] Amongst the four strong absorptions at 1557, 1541, 1444, 1390 cm^{-1} for **2** (1568, 1547, 1429 and 1394 cm^{-1} for **3**, and 1572, 1556, 1439 and 1394 cm^{-1} for **4**), the peaks at 1557 and 1541 cm $^{-1}$ for **2** (1568 and 1547 cm^{-1} for **3**, and 1572 and 1556 cm^{-1} for **4**) are attributed to ν_{as}(COO) of the three complexes. The splitting of the ν_{as}(COO) peak indicates that both carboxylate groups of the ip ligand are in two different coordination modes,[11b] which is consistent with their respective crystal structures. The other two peaks at 1444 and 1390 cm^{-1} for **2** (1429 and 1394 cm^{-1} for **3**, and 1439 and 1394 cm^{-1} for **4**) correspond to ν_s(COO) of the bidentate chelating carboxylate group and the bidentate bridging carboxylate group, respectively.

Description of the Crystal Structures

The X-ray structure determination revealed a novel and complex covalently bonded 2D network for **1**, containing two crystallographically independent manganese(II) ions of different octahedral geometry. As shown in Figure 1 for compound **1**, the ip ligands are of two types: A and B [as shown in Scheme 2 (a) and (b), respectively]. The two crystallographically independent Mn atoms (Mn1 and Mn2), with an interatomic distance of 3.476(2) Å, are bridged by one μ-aqua (Ow), one $\mu_{1,3}$-OCO and one $\mu_{1,1}$-OCO bridge. To the best of our knowledge, this type of triply bridged Mn dimeric core is unique, although three examples containing one μ-aqua and two $\mu_{1,3}$-OCO bridges were previously reported.[12] The bond valence sum (BVS) calculations[13] give the values of 2.00 and 2.11 for Mn1 and Mn2, respectively, indicating that the Mn centers are of +2 oxidation state. In order to maintain the electroneutrality of the compound, the Ow is assigned as a neutral water ligand. Additionally, the absence of characteristic IR absorptions around 1700 cm^{-1} expected for the vibration of protonated carboxyl groups (COOH), indicates that all carboxyl groups in **1** are deprotonated. Furthermore, the Mn−Ow distances of 2.229(2) and 2.331(2) Å fall in the normal range found in other Mn complexes,[12,14] which also suggests that the bridging ligand is water. The Mn1 and Mn2 atoms are coordinated by one N atom of Him, one bridging Ow atom, and two bridging O atoms from the μ_4-ip ligands. Two O atoms of the μ_3-ip ligand chelate to Mn1 and coordinate monodentately to Mn2, respectively, completing the distorted octahedral geometries (Table 1) of the two Mn ions. The Mn_2 unit is further dimerized through two *syn*/*anti*-carboxylate bridges from symmetry-related μ_4-ip ligands to form a novel nonplanar cyclic Mn tetramer containing four Mn octahedra and two carboxylate groups with Mn1···Mn2A = 5.309(2) Å. The most remarkable structural feature of **1** is that each Mn tetramer connects eight ip ligands to form an infinite 2D coordination framework featuring an unprecedented puckered rhombic grid-like $[Mn_{16}(ip)_8(H_2O)_8(Him)_{16}]$ as the basic building block (Figure 2). Each apex of the grid is occupied by a Mn_4 clus-

Table 1. Selected bond lengths [Å] and angles [°] for **1** (symmetry codes: A: $-x + 1, -y + 1, -z + 1$; B: $x + 1, y + 1, z$, C $x, y + 1, z$)

Mn1−O5A	2.090(2)	O5A−Mn1−O1	137.13(8)
Mn1−O7B	2.139(2)	O7B−Mn1−O1	96.64(9)
Mn1−N1	2.196(3)	N1−Mn1−O1	103.58(1)
Mn1−Ow	2.229(2)	Ow−Mn1−O1	78.44(8)
Mn1−O2	2.267(2)	O2−Mn1−O1	55.46(8)
Mn1−O1	2.425(2)	O6−Mn2−O8B	176.91(1)
Mn2−O6	2.082(2)	O6−Mn2−O4C	95.94(1)
Mn2−O8B	2.127(2)	O8B−Mn2−O4C	86.77(1)
Mn2−O4C	2.143(2)	O6−Mn2−N3	91.29(1)
Mn2−N3	2.197(3)	O8B−Mn2−N3	89.63(1)
Mn2−O1	2.312(2)	O4C−Mn2−N3	101.43(1)
Mn2−Ow	2.331(2)	O6−Mn2−O1	96.24(1)
O5A−Mn1−O7B	121.58(1)	O8B−Mn2−O1	80.77(9)
O5A−Mn1−N1	100.13(1)	O4C−Mn2−O1	161.06(9)
O7B−Mn1−N1	82.68(1)	N3−Mn2−O1	92.75(1)
O5A−Mn1−Ow	87.39(9)	O6−Mn2−Ow	90.79(9)
O7B−Mn1−Ow	82.57(9)	O8B−Mn2−Ow	87.88(9)
N1−Mn1−Ow	165.25(1)	O4C−Mn2−Ow	86.58(9)
O5A−Mn1−O2	87.64(9)	N3−Mn2−Ow	171.46(1)
O7B−Mn1−O2	150.72(9)	O1−Mn2−Ow	78.80(8)
N1−Mn1−O2	94.71(1)	Mn2−O1−Mn1	94.36(8)
Ow−Mn1−O2	98.29(9)	Mn1−Ow−Mn2	99.27(9)

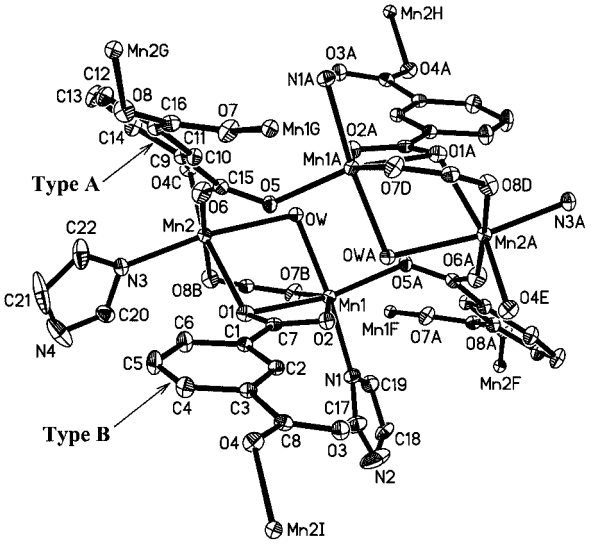

Figure 1. The local coordination environments of the Mn^{2+} centers in **1** (ellipsoids at 30% probability); types A and B indicate two independent ip ligands with different coordination modes

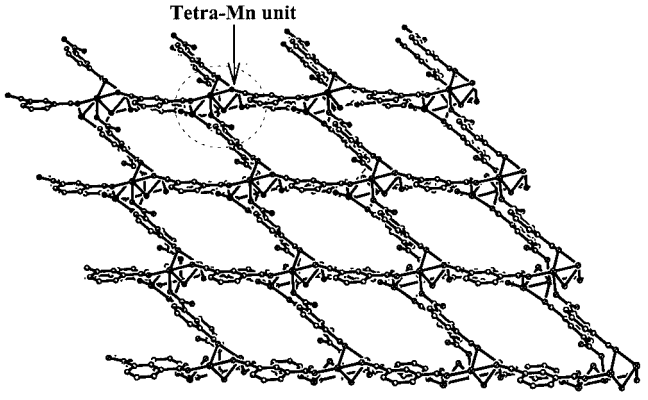

Figure 2. A view of the 2D layer showing rhombic grids in **1**, with the imidazole ligands excluded for clarity

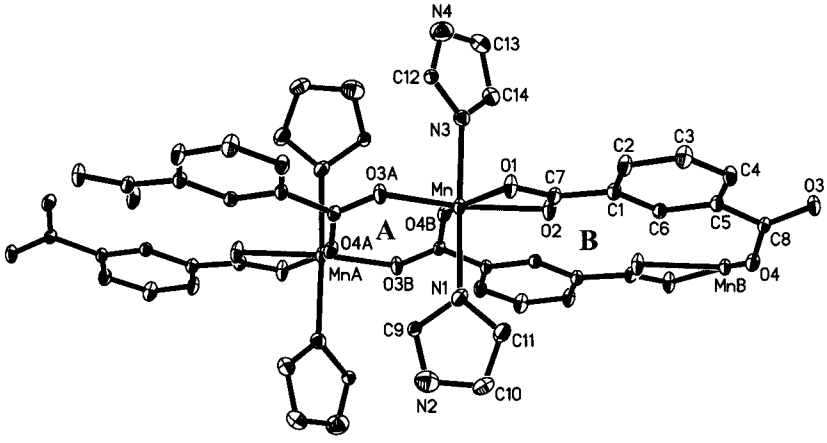

Figure 3. The local coordination environment of the Mn^{2+} center in **2** (ellipsoids at 30% probability); **A** and **B** denote the two subrings contained in the $[Mn_2(\mu\text{-}OCO)_2]$ and $[Mn_2(\mu\text{-}ip)_2]$ moieties, respectively

ter which is surrounded by ip ligands in bridging bis(bidentate) μ_4, bridging/chelating bidentate and monodentate μ_3 modes.

The structure of **2** differs from the structure of **1** since the coordination of water to Mn was completely precluded. Each ip ligand coordinates to three Mn atoms through two carboxylate groups in an interesting bridging and chelating bis(bidentate) μ_3 mode [Scheme 2 (c)] resulting in an infinite 1D polymer. Figure 3 illustrates the distorted octahedral geometry of the Mn^{2+} center (Table 2) with four O atoms from three ip ligands in the equatorial plane, and with two Him N atoms occupying the *trans*-axial positions. One pair of symmetry-related Mn atoms (Mn and MnA) with an interatomic distance of 4.480(2) Å is bridged by two carboxylate groups to produce a four-membered (two octahedra and two carboxylate groups) ring (**A**), whereas the other pair of symmetry-related Mn atoms (Mn and MnB) with an interatomic distance of 7.098(2) Å are bridged by two extended ip ligands to produce another four-membered (two octahedra and two isophthalate groups) ring (**B**). The two types of subrings, **A** and **B**, alternately interlock through Mn−O−C edge-sharing to produce a 1D parallel double chain of $[Mn(ip)]_n$ (with respect to the Mn atoms) in the *c* direction. Interestingly, the capping Him ligands are located at both sides of the double chain (Figure 4), thus preventing a 2D structure for **2**. It is reasonable to expect that a 2D double-layer framework will be created if the Him ligands are replaced by bidentate linear linkers such as 4,4′-bipyridine or (*E*)-1,2-bis(4-pyridyl)ethene.

Table 2. Selected bond lengths [Å] and angles [°] for **2** (symmetry codes: A: $x, y, z - 1$; B: $-x + 1, -y + 2, -z + 2$)

Mn−O3A	2.118(2)	O2−Mn−N1	87.99(1)
Mn−O4B	2.170(2)	O3A−Mn−N3	88.01(1)
Mn−O2	2.181(2)	O4A−Mn−N3	83.76(1)
Mn−N1	2.234(3)	O7B−Mn2−O3	85.96(18)
Mn−N3	2.244(3)	O2−Mn−N3	90.71(1)
Mn−O1	2.342(3)	N1−Mn−N3	171.70(1)
O3A−Mn−O4B	105.41(9)	O3A−Mn−O1	94.42(9)
O1−Mn1−O2A	118.66(2)	O4B−Mn−O1	158.00(1)
O3A−Mn−O2	152.19(1)	O2−Mn−O1	57.77(9)
O4B−Mn−O2	102.05(9)	N1−Mn−O1	98.62(11)
O3A−Mn−N1	96.95(1)	N3−Mn−O1	87.58(11)
O4B−Mn−N1	88.50(1)	N4−Mn2−O4	130.48(18)

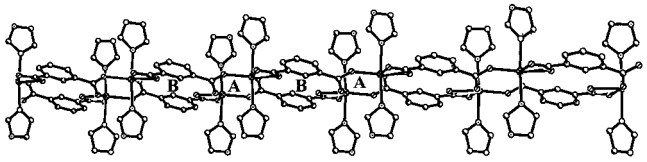

Figure 4. A view of the double-chain framework of **2** showing alternate interlocking of the two types of subrings (**A** and **B**) into parallel double chains of $[Mn(ip)]_n$

Complex **3** was obtained when (*E*)-1,2-bis(4-pyridyl)-ethene (dpe) was used instead of Him in the reaction. As expected, the structure of **3** is an infinite 2D double-layer polymer. The solvate dpe molecule is distorted within the crystal lattice but its presence was confirmed by elemental analysis. However, the neutral polymeric framework is clearly defined. As shown in Figure 5, the coordination mode of the ip ligand is identical to that found in **2**. Again, three ip ligands coordinate equatorially to one Mn atom through four carboxyl O atoms [Mn−O = 2.113(5)−2.329(5) Å] (Table 3), forming a 1D parallel double chain of $[Mn(ip)]_n$ almost the same as that contained in **2**. One remarkable structural feature of **3** is that the adjacent double chains of $[Mn(ip)]_n$ are cross-linked by linear μ-dpe ligands in the axial directions of the Mn octahedra [Mn−N1 = 2.263(5), Mn−N2C = 2.266(6) Å] giving a novel 2D double-layer framework with large open rectangular cavities (Figure 6). The intracavity Mn···Mn separation, bridged through the dpe, the ip and the μ_2-bridging carboxylate group, is 13.919 × 10.178 × 4.028 Å. These layers stack along the crystallographic *a* axis, generating large rectangular channels, which in turn accommodate solvate dpe and water molecules in the crystal lattice (Figure 7).

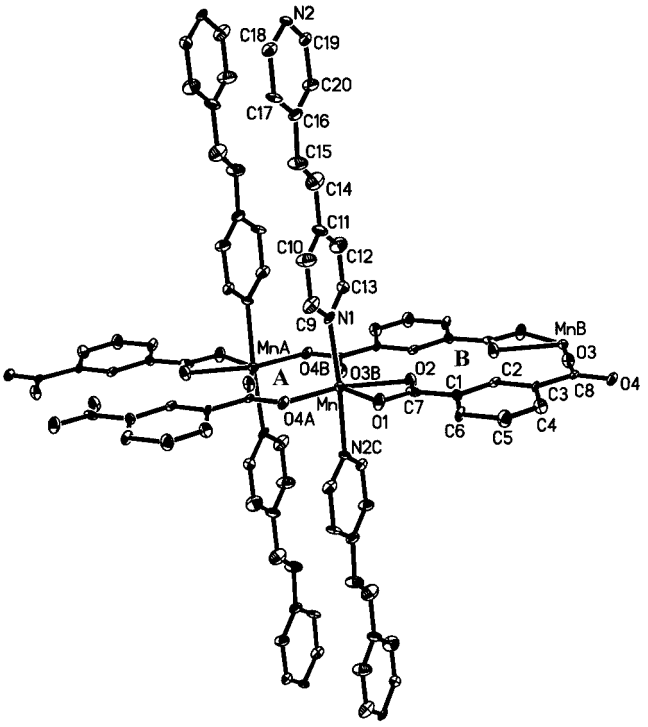

Figure 5. The local coordination environment of the Mn^{2+} center in **3** (ellipsoids at 25% probability); **A** and **B** denote the two subrings similarly to those found in **2**

Table 3. Selected bond lengths [Å] and angles [°] for **3** (symmetry codes: A: $-x + 3, -y - 2, -z - 1$; B: $x, y - 1, z$, C $x + 1, y, z - 1$)

Mn−O4A	2.113(5)	O2−Mn−N1	92.2(2)
Mn−O3B	2.145(5)	O4A−Mn−N2C	87.9(2)
Mn−O2	2.245(4)	O3B−Mn−N2C	87.7(2)
Mn−N1	2.263(5)	O2−Mn−N2C	92.0(2)
Mn−N2C	2.266(6)	N1−Mn−N2C	174.8(2)
Mn−O1	2.329(5)	O4A−Mn−O1	147.76(18)
O4A−Mn−O3B	123.72(19)	O3B−Mn−O1	88.36(17)
O4A−Mn−O2	91.06(18)	O2−Mn−O1	56.80(17)
O3B−Mn−O2	145.16(19)	N1−Mn−O1	94.3(2)
O4A−Mn−N1	89.1(2)	N2C−Mn−O1	90.5(2)
O3B−Mn−N1	90.5(2)		

When 2,2′-bipyridine (bpy) was used instead of Him, complex **4** was obtained. The X-ray structure determination reveals that **4** is a 1D chain-like polymer constructed from $[Mn_2(ip)_2(bpy)_2]$ units. As shown in Figure 8, two symmetry-unrelated ip ligands exhibit two types of coordination mode [shown in Scheme 2 (c) and (d)]. The latter is a bridging bidentate and monodentate μ_3 mode. Several differences in the coordination environments of the two crystallographically distinct Mn^{2+} atoms can be observed (Table 4). The Mn2 atom has a distorted octahedral geometry coordinated by two N and four O atoms, whereas the Mn1 atom is in distorted trigonal-bipyramidal geometry, being coordinated by two N and three O atoms. However, the Mn1···O6 distance of 2.528(5) Å indicates a

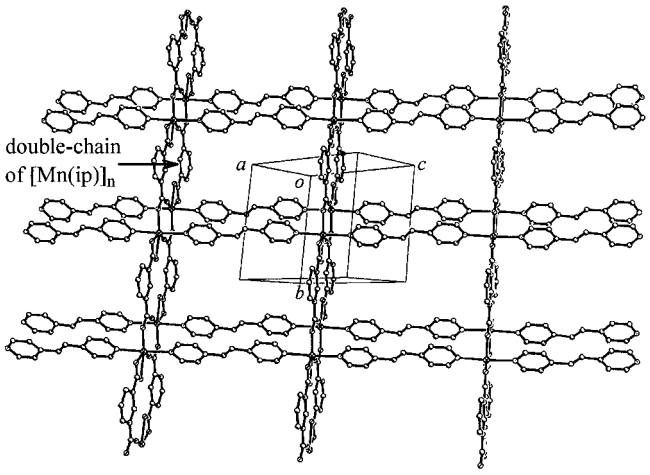

Figure 6. A view of the double-layer framework of **3** showing the μ-dpe bridges between the double-chain of $[Mn(ip)]_n$ and the formation of a rectangular cavity

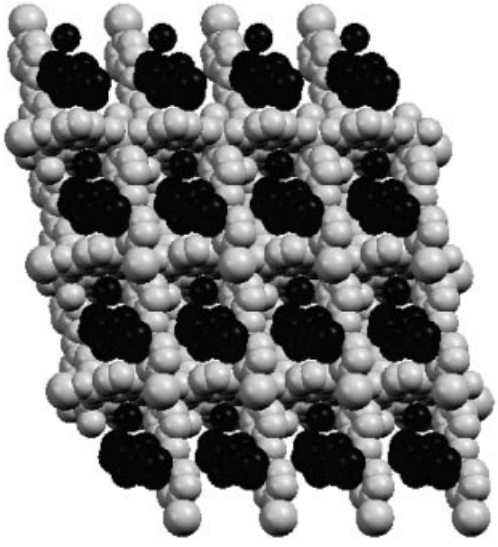

Figure 7. Space-filling diagram of **3** showing solvate molecules (black) contained in the rectangular channels in the *a* direction

weak interaction, which may be described as a semichelating coordination mode of the monodentate carboxylate group.[15] Similarly to **2** and **3**, every three ip ligands coordinate to one Mn atom to produce a 1D double chain of $[Mn_2(ip)_2]_n$ (Figure 9). It is worth noting that the $[Mn_2(ip)_2]_n$ motif, featuring a double-helix chain with a long pitch of about 10 Å, is more distorted than those of $[Mn(ip)]_n$ in **2** and **3** due to *cis* chelation of the rigid bpy ligand to an Mn center. The double chain also differs structurally from that reported previously in an isomeric complex containing an $[Mn(ip)(bpy)]_n$ core,[16] where all Mn atoms were symmetry-dependent, and all carboxyl O atoms were coordinated to Mn centers with all of the Mn−O bond lengths in the usual range [2.111(2)−2.284(3) Å]. Interestingly, the adjacent double-helical chains of **4** were intercalated in a zipper style to form 2D supramolecular layers through the π-π stacking interactions between the

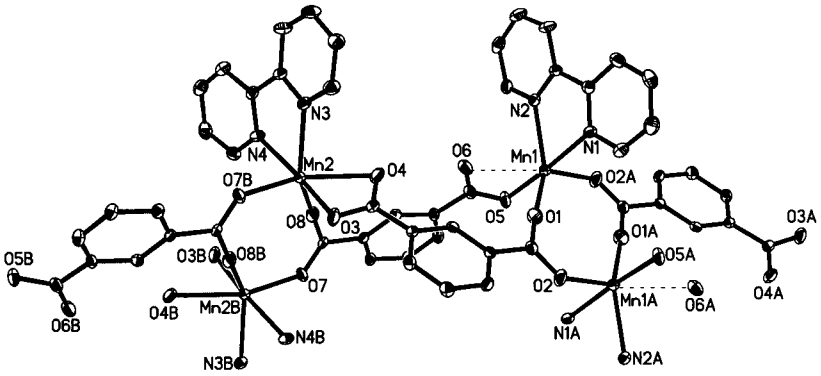

Figure 8. The local coordination environments of the Mn^{2+} centers in **4** (ellipsoids at 30% probability)

Table 4. Selected bond lengths [Å] and angles [°] for **4** (symmetry codes: A: $-x + 1, -y + 1, -z + 1$; B: $-x + 2, -y, -z + 2$)

Mn1−O1	2.101(5)	O2A−Mn1−N1	88.6(2)
Mn1−O2A	2.123(4)	O5−Mn1−N1	174.74(19)
Mn1−O5	2.145(5)	N2−Mn1−N1	72.24(19)
Mn1−N2	2.245(5)	O8−Mn2−O7B	113.05(18)
Mn1−N1	2.273(5)	O8−Mn2−O3	102.2(2)
Mn2−O8	2.094(5)	O7B−Mn2−O3	85.96(18)
Mn2−O7B	2.121(4)	O8−Mn2−N3	136.7(2)
Mn2−O3	2.224(5)	O7B−Mn2−N3	100.57(18)
Mn2−N3	2.276(5)	O3−Mn2−N3	106.8(2)
Mn2−N4	2.322(5)	O8−Mn2−N4	85.02(19)
Mn2−O4	2.393(5)	O7B−Mn2−N4	86.10(19)
O1−Mn1−O2A	118.66(19)	O3−Mn2−N4	170.89(19)
O1−Mn1−O5	96.8(2)	N3−Mn2−N4	70.36(18)
O2A−Mn1−O5	89.63(19)	O8−Mn2−O4	87.41(18)
O1−Mn1−N2	137.7(2)	O7B−Mn2−O4	140.72(18)
O2A−Mn1−N2	98.57(19)	O3−Mn2−O4	56.20(17)
O5−Mn1−N2	103.1(2)	N3−Mn2−O4	82.87(18)
O1−Mn1−N1	88.4(2)	N4−Mn2−O4	130.48(18)

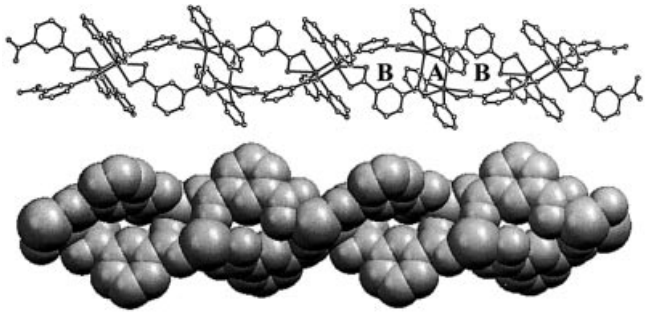

Figure 9. A view of the double-chain structure of **4** (top), **A** and **B** denote the two subrings within the $[Mn_2(\mu\text{-}OCO)_2]$ and $[Mn_2(\mu\text{-}ip)_2]$ moieties, respectively; space-filling diagram of the double-helix structure of **4** with the capping bpy ligands omitted (bottom)

bpy ring planes with face-to-face distances of ca. 3.55−3.68 Å (Figure 10).

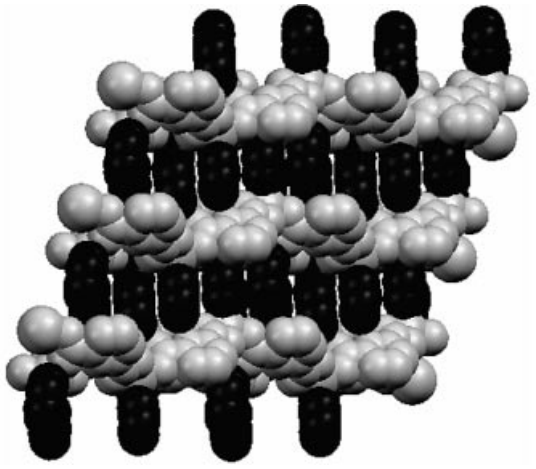

Figure 10. Space-filling diagram of a supramolecular layer in **4** showing the zipper-like intercalation of bpy ligands (black) from adjacent double-chains

Magnetic Susceptibility Study of Compounds

The magnetic behavior of complex **1** is plotted in Figure 11. At room temperature, the experimental effective magnetic moment (μ_{eff}) is 7.93μ_B, which is slightly smaller than the value of 8.37μ_B expected for two uncoupled Mn^{2+} ions (S1 = S2 = 5/2). Upon cooling from room temperature to 80 K, the value of μ_{eff} remains essentially constant, then gradually decreases to 4.24 μ_B at 5 K, indicative of an overall antiferromagnetic coupling between the Mn^{2+} centers.

As indicated in the structure description, **1** is a 2D double-layer polymer built from Mn_4 entities linked by ip ligands. No appropriate analytical expressions were available for calculation of the interaction parameters for this double-layer system. However, magnetic coupling between Mn tetramers through the extended ip bridging ligands and between the mixed water/carboxyl-bridged Mn dimers through the *syn*/*anti*-bridging carboxylate groups are all expected to be very weak. Thus, a simplified analysis of this coupling system can be accomplished by either of two approaches:

(i) The first approach neglects the Mn intertetramer magnetic interactions through the extended ip-bridging ligands. The observed magnetic behavior was simulated using modified Equation (1), which was obtained by combining the dimer model of $S = 5/2$ spins ($\boldsymbol{H} = -2J\boldsymbol{S}_1\boldsymbol{S}_2$)[17] with the Mn interdimeric interactions (zJ') under the molecular field approximation[18] [see inset of Figure 11 (a)].

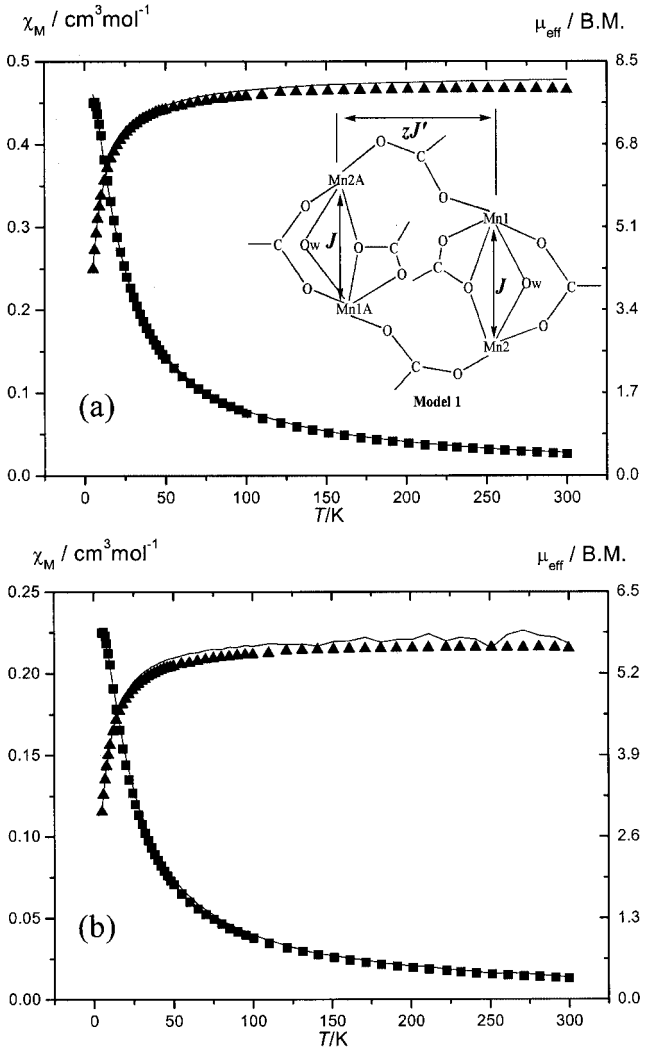

Figure 11. Experimental magnetic susceptibilities (χ_M, marked as square) and effective magnetic moment (μ_{eff}, marked as triangle) as a function of temperature for complex **1**; the solid lines represent the calculated values

$$\chi_M = \chi_{bi}/\left(1 - zJ'\chi_{bi}/Ng^2\beta^2\right)$$

where

$$\chi_{bi} = \frac{2Ng^2\beta^2}{kT}\left[\frac{55+30\exp(-10J/kT)+14\exp(-18J/kT)+5\exp(-24J/kT)+\exp(-28J/kT)}{11+9\exp(-10J/kT)+7\exp(-18J/kT)+5\exp(-24J/kT)+3\exp(-28J/kT)+\exp(-30J/kT)}\right] \quad (1)$$

A best-fit result with parameters $J = -2.16(8)$ cm^{-1}, $zJ' = -0.01(4)$ cm^{-1}, $g = 1.96(9)$, and the agreement factor R [defined as $R = \Sigma[(\chi_M T)_{calcd.} - (\chi_M T)_{obsd.}]^2/[\Sigma(\chi_M T)_{obsd.}]^2 = 1.73 \times 10^{-4}$ was obtained over the temperature range studied.

The small negative zJ' value agrees well with the notion that the *syn*/*anti*-carboxylate bridge always mediates very weak magnetic couplings due to the expanded metallic core and the mismatch in the orientation of magnetic orbitals.[19] The small zJ'/J ratio (ca. 0.006) validates the use of the mean molecular field approximation model.[20]

(ii) In the second approach the magnetic interactions through the *syn*/*anti*-carboxylate bridges were ignored, and the magnetic behavior of **1** was simulated using the analytical expression according to Equation (2) based on the homonuclear alternating chain structure,[21] where $u_i = \coth[J_iS(S+1)/kT] - kT/[J_iS(S+1)]$ $(i = 1, 2)$.

$$\chi = \frac{Ng^2S(S+1)\mu_B^2}{3kT}\left(\frac{1+u_1+u_2+u_1u_2}{1-u_1u_2}\right) \quad (2)$$

The best fit gives the parameters $J_1 = -1.48(4)$ cm^{-1}, $J_2 = -0.01(9)$ cm^{-1}, $g = 1.96(5)$ and $R = 7.99 \times 10^{-4}$ over the temperature range studied.

Although the latter simulation is mathematically logical, the theoretical curve is not smooth in the high-temperature range (100−300 K), which can be seen from Figure 11 (b). On the basis of this, the result derived from the first simulation seems to be more exact for compound **1**.

Complexes **2**, **3** and **4** have similar magnetic properties and the plots of the effective magnetic moment (μ_{eff}) vs. T are shown in Figure 12. At room temperature, the values of μ_{eff} were 5.90 μ_B, 5.88 μ_B and 5.83 μ_B per one Mn^{2+} ion for **2**, **3** and **4**, respectively. These values are close to, or slightly lower than, the value of 5.91 μ_B expected for an "isolated" Mn^{2+} ion ($S = 5/2$). As the temperature is lowered, the μ_{eff} values remain essentially constant in the regions 300−60 K, 300−80 K, and 300−100 K for **2**, **3**, and **4**, respectively. When the temperature is further lowered, the μ_{eff} values decrease continuously down to 4.15 μ_B, 3.54 μ_B and 3.67 μ_B at 5 K for **2**, **3** and **4**, respectively, indicating overall antiferromagnetic couplings between Mn^{2+} centers for the three complexes. Considering that the magnetic interaction between two Mn centers separated by > 14 Å through μ-dpe in **3** is very weak, the analytical expression according to

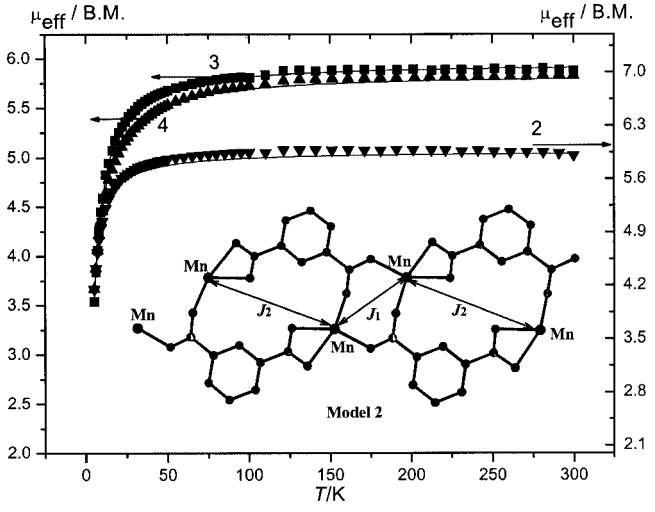

Figure 12. Experimental effective magnetic moment (μ_{eff}) as a function of temperature for complexes **2**−**4**; the solid lines represent the calculated values

Equation (2) for the homonuclear alternating chain structure (see inset of Figure 12) can be adopted to simulate the magnetic behavior of the three complexes.

The least-squares fitting of the experimental data over the full temperature range led to $J_1 = -0.71(4)$ cm^{-1}, $J_2 = -0.02(2)$ cm^{-1}, $g = 2.02(2)$ and the agreement factor $R = 2.10 \times 10^{-4}$ for **2**, $J_1 = -1.01(3)$ cm^{-1}, $J_2 = -0.09(1)$ cm^{-1}, $g = 2.01(1)$ and $R = 6.0 \times 10^{-5}$ for **3**, and $J_1 = -0.80(1)$ cm^{-1}, $J_2 = -0.46(2)$ cm^{-1}, $g = 1.98(2)$ and $R = 8.1 \times 10^{-4}$ for **4**.

All these negative J_1 values fall in the range (-0.7 to -1.84 cm^{-1}) expected for doubly bridged Mn^{2+} carboxylate compounds,[22] and the differences in them [J_1(**3**) > J_1(**4**) > J_1(**2**)] agree well with the inter-Mn distance (4.028 Å for **3**, 4.322 Å for **4** and 4.480 Å for **2**). Shorter separation of paramagnetic centers allows more effective magnetic coupling. For all of the complexes, the smaller negative J_2 value can be attributed to a very weak antiferromagnetic interaction through the extended bridging ip ligand pathway. Its low magnitude can be associated with the excessive span (> 7 Å) of the ip ligand bridge, and is logically smaller than the J_1 value mediated by double carboxylate bridges presenting short pathways.

Conclusion

In this paper, four low-dimensional coordination polymers **1**−**4** have been synthesized by treatment of an Mn^{2+} salt with isophthalic acid and with the participation of selected ancillary ligands − Him, dpe and bpy − under different crystallization conditions. The evolution of structure of these compounds was as expected. Under ambient conditions, the spontaneous assembly of ip and Mn^{2+} salt with the participation of Him ligand yielded the novel 2D double-layer framework **1**. Hydrothermal conditions inhibited coordination of water to the metal atom, as expected, and led to the formation of **2**, which consists of an interesting double-chain framework. Polymer **3**, with a 2D double-layer framework, was rationally induced by the use of secondary μ-dpe ligands as axial connectors of Mn octahedra in double chains of $[Mn(ip)]_n$. The parallel $[Mn(ip)]_n$ double-chain moiety was further modified to the helical double-chain framework in **4** by introduction of the steric constraint caused by *cis* chelation of the rigid bpy ligand. The results show that metal-organic coordination polymers with a specific architecture may be elaborated by the judicious choice of the organic spacer and ancillary ligand, along with careful manipulation of various reaction conditions such as the reaction temperature and solvent. The magnetic properties of these compounds revealed overall weak antiferromagnetic exchange interactions between Mn^{2+} ions through the bridging carboxylate group of the ip ligand or through the extended ip ligand bridge. The coupling interactions, as well as the differences in them, were explained briefly according to the structural parameters and their variations.

Experimental Section

General Remarks: All chemicals were of reagent grade and used as received. Elemental analyses were performed with a Vario EL-III element analyzer. IR spectra of KBr pellets (4000−400 cm^{-1}) were recorded with an FTS-40 spectrophotometer. Variable-temperature magnetic susceptibilities were measured over the temperature range 5−300 K on crystalline samples mounted in a capsule using a model CF-1 superconducting magnetometer. Diamagnetic corrections were estimated with Pascal's constants for all the complexes: -2.50×10^{-4} c.g.s. for **1**, -1.68×10^{-4} c.g.s. for **2**, -2.56×10^{-4} c.g.s. for **3** and -3.55×10^{-4} c.g.s. for **4**.

Synthesis of $[Mn_4(ip)_4(H_2O)_2(Him)_4]_n$ (1): Solid $Mn(OAc)_2{\cdot}4H_2O$ (0.50 g, 2 mmol) was added to an H_2O/MeOH (ca. 4:1, v/v, 20 mL) solvent mixture containing isophthalic acid (H_2ip) (0.34 g, 2 mmol), KOH (0.23 g, 4 mmol) and imidazole (Him) (0.14 g, 2 mmol) with continuous stirring. The solution was stirred at room temperature for 2 h, then filtered. The filtrate was left in a $CaCl_2$ desiccator for approximately one month to produce colorless crystals of **1** in 68% yield (0.41 g). $C_{44}H_{36}Mn_4N_8O_{18}$ (1184.57): calcd. C 44.61, H 3.06, N 9.46; found C 44.69, H 3.14, N 9.44. IR (KBr): $\tilde{\nu}$ = 3320 (br., s), 3080 (m), 1612 (s), 1566 (s), 1520 (m), 1477 (m), 1448 (s), 1394 (s), 1325 (m), 1271(w), 1255 (w), 1157 (w), 1126 (w), 1092 (w), 1070 (m), 1061(s), 935 (w), 906 (w), 856 (w), 837 (w), 820 (m), 744 (s), 712 (s), 704 (s), 658 (s), 619 (m), 538 (w), 459 (w), 434 (m) cm^{-1}.

Synthesis of $[Mn(ip)(Him)_2]_n$ (2): Complex **1** (1.2 g, 1 mmol) was dissolved in an H_2O/MeOH (ca. 4:1, v/v, 15 mL) solvent mixture and was heated at 140 °C in a 20-mL sealed Teflon-lined stainless vessel for 4 d, then cooled to room temperature over a period of 5 h. This gave colorless crystals of **2** in 54% yield (0.77 g). $C_{14}H_{12}MnN_4O_4$ (355.22): calcd. C 47.34, H 3.41, N 15.77; found C 47.37, H 3.49, N 15.72. IR (KBr): $\tilde{\nu}$ = 3064 (m), 1605 (s), 1557 (s), 1541 (s), 1477 (m), 1446 (s), 1444 (s), 1390 (s), 1352 (m), 1311 (w), 1277 (w), 1250 (w), 1178 (w), 1157 (m), 1134 (m), 1119 (s), 1076 (w), 1057 (s), 1041 (s), 939 (m), 908 (m), 877 (m), 827 (w), 816 (w), 780 (s), 746 (s), 715 (s), 658 (w), 611 (m), 573 (w), 532 (w), 451 (w), 432 (m), 408 (m) cm^{-1}.

Synthesis of $[Mn(ip)(dpe)]_n{\cdot}0.5ndpe\cdot nH_2$O (3): $Mn(OAc)_2{\cdot}4H_2O$ (0.25 g, 1 mmol), dissolved in water (10 mL), was mixed with an H_2O/EtOH (ca. 1:1, v/v, 10 mL) solvent mixture containing H_2ip (0.17 g, 1 mmol), KOH (0.11 g, 2 mmol) and dpe (0.28 g, 1.5 mmol) leading to the immediate precipitation of a yellow powder which was filtered. Small yellow crystals of **3**, suitable for X-ray diffraction, were grown from the filtrate upon standing at room temperature for three weeks. Yield: 11% (0.06 g). $C_{26}H_{21}MnN_3O_5$ (510.40): calcd. C 61.18, H 4.15, N 8.23; found C 61.25, H 4.16, N 8.21. IR (KBr): $\tilde{\nu}$ = 3442 (br., s), 3037 (m), 1608 (s), 1568 (s), 1547 (s), 1479 (m), 1429 (s), 1394 (s), 1254 (w), 1217 (m), 1105 (w), 1074 (w), 1014 (s), 972 (m), 912 (w), 827 (s), 746 (s), 719 (s), 660 (w), 552 (s), 509 (w), 424 (m) cm^{-1}.

Synthesis of $[Mn_2(ip)_2(bpy)_2]_n$ (4): 2,2′-bipyridine (bpy) (0.31 g, 2 mmol) in DMF (10 mL) was slowly added to a solution of $Mn(OAc)_2{\cdot}4H_2O$ (0.50 g, 2 mmol), H_2ip (0.34 g, 2 mmol) and NaOH (0.16 g, 4 mmol) in water (25 mL) with continuous stirring, resulting in a yellow suspension. The suspension was transferred into a 50-mL round-bottomed flask and heated to reflux for about a week during which time yellow crystals of **4** deposited in 17% yield (0.13 g). $C_{36}H_{24}Mn_2N_4O_8$ (750.47): calcd. C 57.62, H 3.22, N 7.47; found C 57.69, H 3.17, N 7.38. IR (KBr): $\tilde{\nu}$ = 3053 (m), 1610 (s), 1572 (s), 1556 (s), 1473 (m), 1439 (s), 1394 (s), 1313 (w), 1244

Table 5. Crystallographic data summary for complexes **1**−**4**

	1	**2**	**3**	**4**
Empirical formula	$C_{44}H_{36}Mn_4N_8O_{18}$	$C_{14}H_{12}MnN_4O_4$	$C_{26}H_{21}MnN_3O_5$	$C_{36}H_{24}Mn_2N_4O_8$
Formular mass	1184.57	355.22	510.40	750.47
Space group	$P\bar{1}$	$P\bar{1}$	$P\bar{1}$	$P\bar{1}$
a [Å]	10.4583(4)	8.5166(3)	8.9571(3)	9.4704(2)
b [Å]	10.7926(5)	9.2897(3)	10.1785(5)	10.3376(3)
c [Å]	12.4562(5)	10.2230(3)	13.9174(7)	18.5433(6)
α [°]	91.296(1)	73.463(2)	77.395(2)	74.079(1)
β [°]	109.401(1)	74.541(1)	71.240(2)	86.539(2)
γ [°]	116.898(1)	79.782(1)	77.657(2)	63.571(1)
V [Å^3]	1157.40(8)	742.78(4)	1158.24(9)	1559.30(8)
Z	1	2	2	2
T [K]	293(2)	293(2)	293(2)	293(2)
$D_{calcd.}$ [g cm^{-3}]	1.700	1.588	1.463	1.598
μ [mm^{-1}]	1.153	0.915	0.614	0.873
R[a]/wR[b]	0.0387/0.0935	0.0468/0.1308	0.0878/0.1928	0.0782/0.1484

[a] $R = \|\|F_o| - |F_c\|\|/|F_o|$. [b] $Rw = [w(|F_o| - |F_c|)^2/wF_o^2]^{1/2}$.

(m), 1155 (w), 1103 (w), 1076 (w), 1059 (w), 1016 (m), 827 (w), 756 (s), 737 (m), 715 (s), 687 (w), 650 (w), 627 (w), 521 (w), 415 (m) cm^{-1}.

X-ray Crystallographic Study: Intensity data were collected at 293 K with a Siemens SMART CCD diffractometer equipped with a graphite-monochromated Mo-K_α radiation source (λ = 0.71073 Å). Data were corrected for LP factors and empirical absorption correction was applied. Structures were solved by direct methods and refined by full-matrix least-squares refinement on F^2 using the SHELXTL-97 program package.[23] All non-hydrogen atoms were refined anisotropically, and hydrogen atoms were introduced geometrically with the exception of the water hydrogen atoms which were located from the difference Fourier syntheses. The free solvate dpe molecule in **3** was distorted in the lattice because of relatively poor crystal quality and so no attempt was made to refine the hydrogen atoms contained in it. Crystallographic data of **1**−**4** are outlined in Table 5. CCDC-220080 to -220083 contain the supplementary crystallographic data of **1**−**4** for this paper. These data can be obtained free of charge at www.ccdc.cam.ac.uk/conts/retrieving.html [or from the Cambridge Crystallographic Data Centre, 12 Union Road, Cambridge CB2 1EZ, UK; Fax: (internat.) + 44-1223-336-033; E-mail: deposit@ccdc.cam.ac.uk].

Acknowledgments

This work was supported by the NNSFC (No. 30170229), the State Key Basic Research and Development Plan of China (G1998010100, 001CB108906), and the Special Project of the Ministry of Science and Technology of China (2001CCA02500).

[1] [1a] *Magnetism: Molecules to Materials* (Eds.: J. S. Miller, M. Drillon), Wiley-VCH, Weinheim, **2002**, vol. 3. [1b] D. Gatteschi, O. Kahn, J. S. Miller, F. Palacio, *Magnetic Molecular Materials*, NATO ASI Series, Series E, Kluwer Academic Publishers, Dordrecht, The Netherlands, **1991**, vol. 198.

[2] [2a] H. O. Stumpf, L. Ouahab, Y. Pei, D. Grandjean, O. Kahn, *Science* **1993**, *261*, 447−449. [2b] S. Konar, P. S. Mukherjee, E. Zangrando, F. Lloret, R. N. Chaudhuri, *Angew. Chem. Int. Ed.* **2002**, *41*, 1561−1563. [2c] H. Miyasaka, N. Matsumoto, H. Okawa, N. Re, E. Gallo, C. Floriani, *J. Am. Chem. Soc.* **1996**, *118*, 981−994. [2d] E. W. Lee, Y. Kim, D.-Y. Jung, *Inorg. Chem.* **2002**, *41*, 501−506. [2e] J. S. Miller, A. J. Epstein, *Angew. Chem. Int. Ed. Engl.* **1994**, *33*, 385−415. [2f] J. Kim, J. M. Lim, Y. K. Choi, Y. K. Do, *Angew. Chem. Int. Ed. Engl.* **1996**, *35*, 998−1000. [2g] N. Guillou, S. Pastre, C. Livage, G. Férey, *Chem. Commun.* **2002**, 2358−2359.

[3] [3a] C. T. Chen, K. S. Suslick, *Coord. Chem. Rev.* **1993**, *128*, 293−322. [3b] S. D. Cox, T. E. Gier, G. D. Stucky, J. Bierlein, *J. Am. Chem. Soc.* **1998**, *110*, 2986−2987. [3c] M. Monfort, I. Resino, J. Ribas, X. Solans, M. Font-Bardia, P. Rabu, M. Drillon, *Inorg. Chem.* **2000**, *39*, 2572−2576. [3d] G. S. Matouzenko, G. Molnar, N. Brefuel, M. Perrin, A. Bousseksou, S. A. Borshch, *Chem. Mater.* **2003**, *15*, 550−556. [3e] *Extended Linear chain compounds* (Ed.: J. S. Miller), Plenum, New York, **1982**, vol. 3.

[4] [4a] J. Cano, G. D. Munno, J. L. Sanz, R. Ruiz, J. Faus, F. Lloret, M. Julve, A. Caneschi, *J. Chem. Soc., Dalton Trans.* **1997**, 1915−1523, and references cited therein. [4b] D.-F. Sun, R. Cao, Y.-C. Liang, Q. Shi, W.-P. Su, M.-C. Hong, *J. Chem. Soc., Dalton Trans.* **2001**, 2335−2340. [4c] C. S. Hong, Y. Do, *Inorg. Chem.* **1997**, *36*, 5684−5685. [4d] J. Cano, G. Demunno, J. Sanz, R. Ruiz, F. Lloret, J. Faus, M. Julve, *J. Chem. Soc., Dalton Trans.* **1994**, 3465−3469. [4e] D.-F. Xiang, X.-S. Tan, Q.-W. Hang, W.-X. Tang, B.-M. Wu, T. C. W. Mak, *Inorg. Chim. Acta* **1998**, *277*, 21−25. [4f] L.-C. Li, D.-Z. Liao, Z.-H. Jiang, S.-P. Yan, *Inorg. Chem.* **2002**, *41*, 421−424. [4g] K. S. Bürger, P. Chaudhuri, K. Wieghardt, B. Nuber, *Chem. Eur. J.* **1995**, *1*, 583−593.

[5] [5a] X.-S. Tan, J. Sun, D.-F. Xiang, W.-X. Tang, *Inorg. Chim. Acta* **1997**, *255*, 157−161. [5b] X.-S. Tan, D.-F. Xiang, W.-X. Tang, K.-B. Yu, *Polyhedron* **1997**, *16*, 1411−1415. [5c] H.-X. Zhang, B.-S. Kang, A.-W. Xu, Z.-N. Chen, Z.-Y. Zhou, A. S. C. Chan, K.-B. Yu, C. Chen, *J. Chem. Soc., Dalton Trans.* **2001**, 2559−2566.

[6] [6a] E. K. Shakhatreh, E. G. Bakalbassis, I. Brudgam, H. Hartl, J. Mrozinski, C. A. Tsipis, *Inorg. Chem.* **1991**, *30*, 2801−2806. [6b] Z.-N. Chen, H.-X. Zhang, K.-B. Yu, B.-S. Kang, H. Cai, C.-Y. Su, T.-W. Wang, Z.-L. Lu, *Inorg. Chem.* **1998**, *37*, 4775−4781.

[7] [7a] K. Wieghardt, *Angew. Chem. Int. Ed. Engl.* **1989**, *28*, 1153−1172. [7b] N. A. Law, M. T. Caudle, V. L. Pecoraro, *Adv. Inorg. Chem.* **1999**, *46*, 305−440.

[8] [8a] C.-B. Ma, C.-N. Chen, Q.-T. Liu, F. Chen, D.-Z. Liao, L.-C. Li, L.-C. Sun, *Eur. J. Inorg. Chem.* **2003**, 2872−2879. [8b] C.-B. Ma, C.-N. Chen, Q.-T. Liu, D.-Z. Liao, L.-C. Li, L.-C. Sun, *New J. Chem.* **2003**, *27*, 890−894. [8c] C.-B. Ma, C.-N. Chen, Q.-T. Liu, D.-Z. Liao, L.-C. Li, *Eur. J. Inorg. Chem.* **2003**, 1227−1231.

[9] [9a] M. Devereux, M. McCann, V. Leon, M. Geraghty, V. McKee, J. Wikaira, *Met.-Based Drugs* **2000**, *7*, 275−278. [9b] S. A. Bourne, J. J. Lu, A. Mondal, B. Moulton, M. J. Zaworotko, *Angew. Chem. Int. Ed.* **2001**, *40*, 2111−2113. [9c] S. A. Bourne, A. Mondal, M. J. Zaworotko, *Cryst. Eng.* **2001**, *4*, 25−36.

[10] [10a] Y. Kim, D.-Y. Jung, *Inorg. Chem.* **2000**, *39*, 1470−1475. [10b] S. O. H. Gutschke, M. Molinier, A. K. Powell, R. E. P. Winpenny, P. T. Wood, *Chem. Commun.* **1996**, 823−824. [10c] O. M. Yaghi, H. Li, T. L. Groy, *J. Am. Chem. Soc.* **1996**, *118*, 9096−9097. [10d] R. Kuhlman, G. L. Schimek, J. W. Kolis, *Inorg. Chem.* **1999**, *38*, 194−196. [10e] C. Livage, C. Egger, G. Ferey, *Chem. Mater.* **1999**, *11*, 1546−1550.

[11] [11a] G. B. Deacon, R. J. Philips, *Coord. Chem. Rev.* **1980**, *33*, 227−250. [11b] K. Nakamoto, *Infrared and Raman Spectra of Inorganic and Coordination Compounds*, John Wiley & Sons, New York, **1986**.

[12] [12a] S.-B. Yu, S. J. Lippard, I. Shweky, A. Bino, *Inorg. Chem.* **1992**, *31*, 3502−3504. [12b] A. Caneschi, F. Ferraro, D. Gatteschi, M. C. Melandri, P. Rey, R. Sessoli, *Angew. Chem. Int. Ed. Engl.* **1989**, *28*, 1365−1367.

[13] [13a] H. H. Thorp, *Inorg. Chem.* **1992**, *31*, 1585−1588. [13b] I. D. Brown, D. Altermatt, *Acta Crystallogr., Sect. B* **1985**, *41*, 244−247.

[14] [14a] T. Lis, *Acta Crystallogr., Sect. B* **1977**, *33*, 2964−2967. [14b] B.-H. Ye, T. Mak, I. D. Williams, X.-Y. Li, *Chem. Commun.* **1997**, 1813−1814. [14c] B. Paluchowska, J. K. Maurin, J. Leciejewicz, *J. Coord. Chem.* **2000**, *51*, 335−347.

[15] [15a] G. Guilera, J. W. Steed, *Chem. Commun.* **1999**, 1563−1564. [15b] J. Tao, M.-L. Tong, X.-M. Chen, *J. Chem. Soc., Dalton Trans.* **2000**, 3669−3674.

[16] M.-L. Hu, D.-J. Xu, D.-P. Cheng, *J. Coord. Chem.* **2002**, *55*, 11−16.

[17] O. Kahn, *Molecular Magnetism*, VCH Publishers Inc., New York, **1993**.

[18] [18a] R. L. Carlin, *Magnetochemistry*, Spinger-Verlag, Berlin, **1986**. [18b]B. E. Myers, L. Berger, S. A. Friedberg, *J. Appl. Phys.* **1969**, *40*, 1149−1151.

[19] [19a] T. K. Maji, S. Sain, G. Mostafa, T.-H. Lu, J. Ribas, M. Monfort, N. R. Chaudhuri, *Inorg. Chem.* **2003**, *42*, 709−716. [19b] D. K. Towle, S. K. Hoffmann, W. E. Hatfield, P. Singh, P. Chaudhuri, *Inorg. Chem.* **1988**, *27*, 394−399. [19c] E. Colacio, J. M. Dominguez-Vera, J.-P. Costés, R. Kivekäs, J. P. Laurent, J. Ruiz, M. Sundberg, *Inorg. Chem.* **1992**, *31*, 774−778. [19d] C. Policar, F. Lambert, M. Cesario, I. Morgenstern-Badarau, *Eur. J. Inorg. Chem.* **1999**, 2201−2207. [19e] R. L. Carlin, K. Kopinga, O. Kahn, M. Verdaguer, *Inorg. Chem.* **1985**, *25*, 1786−1789.

[20] [20a] D. K. Towle, S. K. Hoffmann, W. E. Hatfield, P. Singh, P. Chaudhuri, *Inorg. Chem.* **1988**, *27*, 394−399. [20b] B. Chiari, A. Cinti, L. David, F. Ferraro, D. Gatteschi, O. Piovesana, P. F. Zanazzi, *Inorg. Chem.* **1996**, *35*, 7413−7418.

[21] R. Cortés, M. Drillon, X. Solans, L. Lezama, T. Rojo, *Inorg. Chem.* **1997**, *36*, 677−683.

[22] [22a] P. S. Mukherjee, S. Konar, E. Zangrando, T. Mallah, J. Ribas, N. R. Chaudhuri, *Inorg. Chem.* **2003**, *42*, 2695−2703. [22b] J. Cano, G. D. Munno, J. L. Sanz, R. Ruiz, J. Faus, F. Lloret, M. Julve, A. Caneschi, *J. Chem. Soc., Dalton Trans.* **1997**, 1915−1923. [22c] H. Oshio, E. Ino, I. Mogi, T. Ito, *Inorg. Chem.* **1993**, *32*, 5697−5703. [22d] W.-B. Lin, M. E. Chapman, Z.-Y. Wang, G. T. Yee, *Inorg. Chem.* **2000**, *39*, 4169−4173. [22e] B. Albela, M. Corbella, J. Ribas, I. Castro, J. Sletten, H. Stoeckli-Evans, *Inorg. Chem.* **1998**, *37*, 788−798. [22f] G. Fernández, M. Corbella, J. Mahia, M. A. Maestro, *Eur. J. Inorg. Chem.* **2002**, 2502−2510, and references cited therein.

[23] G. M. Sheldrick, *SHELXL-97*, University of Göttingen, **1997**.

Received February 6, 2004
Early View Article
Published Online June 11, 2004

